Temporal Variations of H_2, H_2O and CH_4 in the Lunar Exosphere driven by Solar Wind Implantation and Impact Vaporization. O.J. Tucker[1], J.L. McLain[1], W.M. Farrell[1], D.M. Hurley[2] ([1]NASA Goddard Space Flight Center, 20771, [2]Greenbelt, Maryland, Johns Hopkins University Applied Physics Lab, 20723, Laurel, Maryland)

Introduction: Hydrogenated molecules (H_2O, OH, H_2, CH_4) have been observed throughout the lunar surface and exosphere. The primary sources for these molecules are solar wind implantation (SWI) and impact vaporization (IV) from meteoroids. However, the relative inventories of these chemically evolved species and production pathways are not well constrained. For example, the source of exospheric water from exogenous sources (SWI & IV) (1, 2) compared to an endogenous desiccated subsurface layer is currently under investigation (3). Likewise, the fraction of the SWI inventory is converted to H_2 (4, 5) versus water (1, 6) is not well constrained. Lastly, CH_4 is another species also evolved from both SWI and IV. Numerical modeling of the temporal variation of the evolved species can provide important constrained on the governing dynamics. Here we examine temporal variabilities of exospheric H_2, H_2O and CH_4 as a function SWI and IV using a global Monte Carlo model (5), and report on results of the evolved mass distribution of ejecta molecules from flash desorption experiments.

Water products have been observed within permanently shadowed regions (PSRs) (7–9) and widespread throughout sunlight regions (10–12). Both surface spectra obtained by Chandrayaan-I Moon Mineralogy Mapper (M^3) and the Lunar Reconnaissance Orbiter Lyman-Alpha Mapping Project LRO-LAMP indicate that surface hydration varies with time of day. However, connecting water products in the exosphere to known surface reservoirs (hydrogen within the top monolayers of grains and within PSRs) is not well characterized. Here we examine the augmentation of the hydrogenated exosphere over a lunation including the variation in the SW proton flux through the traversal of the magnetotail (13) and temporal variations induced during meteoroid streams. For IV we use experimental results of the evolved gases produced during flash desorption experiments of the Apollo Soil 78421 tracked in the global Monte Carlo exosphere model.

Water exosphere: Lunar Atmosphere and Dust Environment Explorer Neutral Mass Spectrometer (LADEE-NMS) measurements of OH/H_2O in the exosphere have been correlated to meteoroid streams which produced temporal median densities of 22.8 mol cm^{-3} (3). However, the steady state exosphere produced from SWI the LADEE-NMS data are indicative of a much lower limit of 0.69 cm^{-3}. This observation is inconsistent with desorption rates inferred from the temporal variation of surface hydration observed by LRO-LAMP (6) and M^3 (14, 15). We will present modeling results for OH/H_2O in the exosphere produced by thermal desorption and micrometeoroid impact to examine the relative contributions concomitantly.

H_2 exosphere: Currently, H_2 is the dominant hydrogen bearing molecule to be observed in the steady-state lunar exosphere. LRO-LAMP measurements were used to derive H_2 surface densities of 1000 ± 500 cm^{-3} and 1400 ± 500 cm^{-3} the dusk and dawn terminators, respectively (16), and the Chandrayaan Chandra Altitudinal Composition Explorer (CHACE) mass spectrometer measured H_2 abundances in the magnetotail consistent with surface densities of 500 – 800 cm^{-3} over latitudes of 20 – 80 degrees, respectively (17). Both measurements are consistent with the H_2 exosphere being derived from the solar wind (18, 19). However, H_2 is also released during impacts as indicated by the Lunar Crater Observation and Sensing Satellite (LCROSS) experiment (18, 20), and in the preliminary flash desorption experiments. Hurley et al. (2015) showed that micrometeoroid impacts are an insufficient source to produce the averaged LAMP observations. However, while in the magnetotail the source H_2 from IV may dominate SWI during meteoroid streams (comparing Figs 1 & 2). To this end predictions of the H_2 distribution in the magnetotail due to IV is useful for observational analyses.

CH_4 exosphere: Hodges et al. (2015) modeled LADEE-NMS data of exospheric CH_4 produced by SWI extracting a post sunrise bulge peaking at ~450 cm^{-3} at 14 km above the surface. The bulge was due to the release of CH_4 molecules adsorbed on the night side release after sunrise. Here we build upon this work by examining the adsorbed CH_4 concentration as a function of latitude, examine the role of C atom diffusion on CH_4 degassing rates and include an IV source based on our flash desorption experiments.

Methods: The mean SWI proton flux in/out of the magnetotail and in the magnetosheath, as well as experimentally derived mass spectra from flash desorption experiments will be used to track the volatized (H_2, CH_4, H_2O and OH) in a global Monte Carlo model. We will adopt the micrometeoroid mass loss rates from Hurley et al. (2015) and references therein and OH/H_2O desorption rates inferred from LAMP (6). IV released sources will be released assuming an impact temperature of T = 1000 -1500 K (Maxwellian) consistent with the flash desorption experiments. The lifetime against photo-destruction of

molecules in the exosphere are adopted from Huebner et al. (2015) (21).

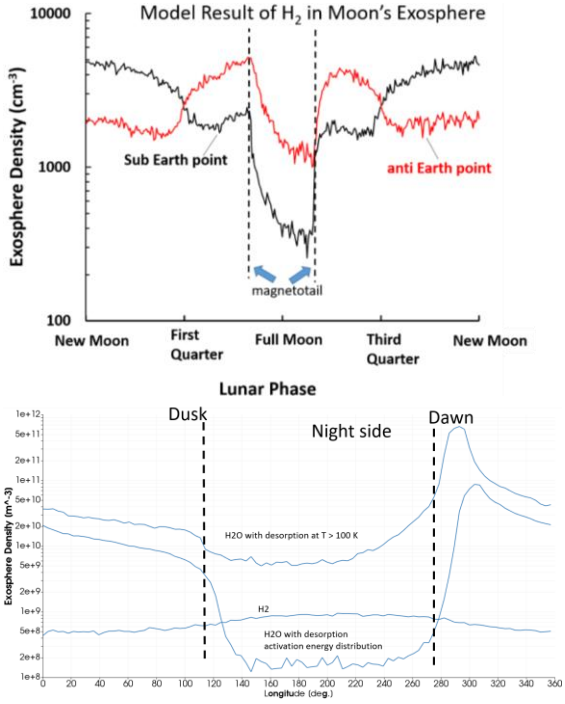

Figure 1: (a) Modeled H_2 exospheric density at sub and anti Earth points as a function of lunation. The dashed line indicates the average time spent in the magnetotail. (b) IV exospheric densities for H_2, H_2O desorption at T > 100 K and H_2O desorption using a distribution of activation energies (densities in units of m^{-3}) as a function of lunar local time where the dashed lines indicate dusk and dawn. IV released H_2 comparable to SWI densities in the magnetotail. Note the location of exospheric bulges near the terminator can provide insight on activation energies for molecular adsorption.

Results: In Figure 1, we show preliminary result of the steady state H_2 equatorial exospheric densities due to SWI implantation (1a) over a lunation, and due to IV (1b) as a function of local time. Note the IV exospheric densities are comparable to SWI while in the magnetotail. Our presentation will review the temporal and global evolution of gases after meteoroid impact, and present results of the mass fraction of evolved species from flash desorption experiments. Tracking the evolution of impact released volatiles over the lunar cycle will enable us to determine expected observational signatures which can be used to test theory.

References: [**1**] Jones BM, Aleksandrov A, Hibbitts K, Dyar MD, Orlando TM. 2018. *Geophys. Res. Lett.* 45(20):10,959-10,967, [**2**] Hurley DM, Cook JC, Retherford KD, Greathouse T, Gladstone GR, et al. 2017. *Icarus*. 283:31–37, [**3**] Benna M, Hurley DM, Stubbs TJ, Mahaffy PR, Elphic RC. 2019. *Nat. Geosci.* 12(5):333–38. [**4**] Hurley DM, Perry ME, Waite JH. 2015. , pp. 1763–73, [**5**] Tucker OJ, Farrell WM, Killen RM, Hurley DM. 2019. *J. Geophys. Res. Planets*. 124(2):278–93, [**6**] Hendrix AR, Hurley DM, Farrell WM, Greenhagen BT, Hayne PO, et al. 2019. *Geophys. Res. Lett.* 46(5):2417–24, [**7**] Hayne PO, Hendrix A, Sefton-Nash E, Siegler MA, Lucey PG, et al. 2015. *Icarus*. 255:58–69, [**8**] Colaprete A, Schultz P, Heldmann J, Wooden D, Shirley M, et al. 2010. *Science (80-.).* 330(6003):463–68, [**9**] Feldman WC, Lawrence DJ, Elphic RC, Barraclough BL, Maurice S, et al. 2000. *J. Geophys. Res. E Planets*. 105(E2):4175–95, [**10**] McCord TB, Taylor LA, Combe JP, Kramer G, Pieters CM, et al. 2011. *J. Geophys. Res. E Planets*. 116(4):1–22, [**11**] Wöhler C, Grumpe A, Berezhnoy AA, Shevchenko V V. 2017. *Sci. Adv.* 3(9):1–11, [**12**] Honniball CI, Lucey PG, Li S, Shenoy S, Orlando TM, et al. 2020. *Nat. Astron.*, [**13**] Tucker OJ, Farrell WM, Poppe AR. 2021. *J. Geophys. Res. Planets*. 126(2), [**14**] Li S, Milliken RE. 2017. *Sci. Adv.* 3(9):1–12, [**15**] Jones BM, Sarantos M, Orlando TM. 2020. *Astrophys. J.* 891(2):L43, [**16**] Cook JC, Stern SA, Feldman PD, Gladstone GR, Retherford KD, Tsang CCC. 2013. *Icarus*. 225(1):681–87, [**17**] Thampi S V., Sridharan R, Das TP, Ahmed SM, Kamalakar JA, Bhardwaj A. 2015. *Planet. Space Sci.* 106:142–47, [**18**] Crider DH, Vondrak RR. 2000. *J. Geophys. Res. E Planets*. 105(E11):26773–82,[**19**] Tucker OJ, Farrell WM, Killen RM, Hurley DM. 2019. *J. Geophys. Res. Planets*. 124(2), [**20**] Hurley DM, Gladstone GR, Stern SA, Retherford KD, Feldman PD, et al. 2012. *J. Geophys. Res. E Planets*. 117(2):1–15, [**21**] Huebner WF, Mukherjee J. 2015. *Planet. Space Sci.*

Acknowledgements: Tucker and McLain acknowledge support for NASA internal science funding GSFC FLaRE and EIMM programs. Farrell and Hurley acknowledge support from SSERVI LEADER.